IEEE Access
Multidisciplinary ⋮ Rapid Review ⋮ Open Access Journal

Received 25 October 2023, accepted 19 November 2023, date of publication 27 November 2023,
date of current version 12 December 2023.

Digital Object Identifier 10.1109/ACCESS.2023.3337046

RESEARCH ARTICLE

A Novel Lane-Change Decision-Making With Long-Time Trajectory Prediction for Autonomous Vehicle

XUDONG WANG[1], JIBIN HU[1], CHAO WEI[1], LUHAO LI[2], YONGLIANG LI[2], AND MIAOMIAO DU[2]

[1]National Key Laboratory of Special Vehicle Design and Manufacturing Integration Technology, Beijing Institute of Technology, Beijing 100081, China
[2]Technology Research and Development Center of eDrive Special Vehicles, Beijing Institute of Space Launch Technology, Beijing 100076, China

Corresponding author: Chao Wei (weipeter1@bit.edu.cn)

ABSTRACT In the process of autonomous vehicle lane changing, a reliable decision-making system is crucial for driving safety and comfort. However, traditional decision-making systems have short-term characteristics, which makes them susceptible to real-time inference from surrounding vehicles. Usually, system sacrifices driving comfort to ensure the safety of the lane change. Balancing driving safety and comfort has always been a research challenge. Long-term trajectory prediction can provide accurate future trajectories of target vehicles, providing reliable long-term information to compensate for the short-term variability of decision systems. This paper proposes a novel decision-making model with long-term trajectory prediction for lane-changing. First, we constructed a long-term trajectory prediction model to predict the trajectories of surrounding vehicles. Besides, we built a lane change decision-making model based on fuzzy inferencing, considering the predicted trajectories to infer the relative relationship between other vehicles and the self-driving car. The establishment of the fuzzy rule library considered the vehicle speed, acceleration, system delay time, driver delay time and the distance between vehicles. Finally, we created a dataset for training and testing the trajectory prediction model, and we built 4 cases simulation environments, for two or three vehicles on a straight road or curved road, respectively, to test the decision-making model. Experimental results show that our proposed model can ensure driving safety and improve driving comfort.

INDEX TERMS Autonomous vehicle, trajectory prediction, decision-making, driving safety, driving comfort.

I. INTRODUCTION

In recent years, autonomous driving technologies have been rapidly developed and have shown great potential in improving traffic efficiency, driving safety, and driving comfort [1], [2], [3]. However, ensuring driving safety is always the primary concern for autonomous vehicles [4], which usually sacrifice driving comfort to ensure safety. This is particularly evident during lane-changing maneuvers, where the autonomous vehicle may prioritize safety over comfort, leading to discomfort and discomfort-related issues for passengers, such as motion sickness. Therefore, improving driving comfort while maintaining safety is an essential goal for autonomous driving research [5], [6].

Although many decision-making models have incorporated prediction modules, decision-making tasks need to employ nonlinear logical reasoning while maintaining interpretability. The current status of vehicles is short-term, and considering it during modeling brings inference difficulties that can lower driving comfort [7]. In contrast, vehicle trajectory [8], [9] is generated by drivers considering traffic rules, maps, and vehicle kinematics. Long-term trajectories provide a basis for decision-making systems to consider long-term trajectory states of the vehicle.

Therefore, this paper proposes a decision-making model for lane change with long-term trajectory prediction. We propose a decision-making model that takes into account

The associate editor coordinating the review of this manuscript and approving it for publication was Shaohua Wan.

long-term trajectory prediction to enhance driving comfort [10] while maintaining safety during lane-changing maneuvers [11], [12], [13]. The main contributions of this paper as follows: Firstly, we propose a trajectory prediction model that differs from most trajectory prediction studies as our designed model involves weight training for specific scenarios that accurately predicts the vehicle's trajectory position. This benefits the specific scenario, which involves vehicle lane changing decision-making tasks. Secondly, we design a decision-making model that considers long-term trajectory prediction. This model uses future trajectory position of surrounding vehicles, the relative position of vehicles, speed, acceleration and the delay time parameters as references. Thirdly, we built a series of simulation driving environment with 4 different cases - straight and curved roads with one or two obstacle vehicles, respectively. We carried out simulation tests to validate the effectiveness of our proposed model.

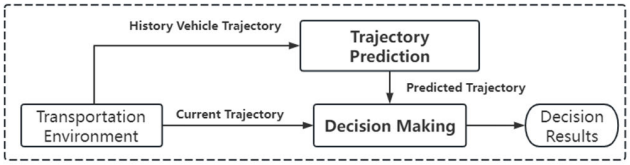

FIGURE 1. Scheme of our proposed method.

The remainder of this paper is organized as follows: Section II introduces the related work. Section III introduces the designing details of proposed method, including LSTM&GRU based trajectory prediction model and Fuzzy inference-based decision-making model. Section IV carries out simulation and analysis on the proposed model through 4 typical driving cases.

II. RELATED WORK

Human drivers have natural ability when changing lanes, which first estimates the possible future position of the obstacle vehicle as a reference for lane-changing decisions, and then selects the appropriate decision time considering safety and comfort. Inspired by the decision logic of human drivers, we proposed a model architecture. Firstly, the trajectory prediction method based on LSTM&GRU requires the vehicle's trajectory history as input and outputs the predicted trajectory in accordance with the temporal order. Specifically, the development and training of the prediction network requires the use of dataset collected from special scenarios. Secondly, the decision algorithm is modeled as a nonlinear fuzzy reasoning problem that considers future trajectory. The prior input of the decision model is the predicted trajectory and the current state information of the vehicle. Decision results are produced through the encoding, rule library, and decoding of the decision model. Finally, the proposed method is verified and analyzed in simulated driving scenario cases.

A. TRAJECTORY PREDICTION

Trajectory prediction plays an important role in ensuring the safety of autonomous vehicles [14]. In recent years, many methods have been applied to predict the future trajectory of vehicles or pedestrians.

The traditional method for trajectory prediction is through physical models that characterize the state of a vehicle directly. Such methods are widely used for dynamic models [15] and kinematic models [16]. In [15], a linear single-vehicle model is employed to avoid collisions, while in [16], it is used for path prediction in connected vehicles. The advantages of such models are their computational efficiency. However, they are often more effective for short-term predictions and are not reliable for long-term predictions.

In contrast, learning-based methods have become the mainstream branch of research in long-term trajectory prediction. Reference [17] proposed a GAN model that combines LSTM and CNN with an attention mechanism for generating obstacle avoidance trajectories in low-speed pedestrian scenarios. GAN models have a burdensome training process [18], and for traffic scenes with higher speeds, various information from maps needs to be added, making the training process more difficult. Recursive neural networks have proven to be efficient in solving sequence prediction tasks [19], [20], [21], [22]. Furthermore, some works have improved the performance of trajectory prediction tasks in complex interactive scenarios by incorporating attention mechanisms [23], [24], [25], [26], [27], [28], [29].

References [30] and [31] propose a trajectory prediction model that combines VAE and LSTM, and [32] established a trajectory prediction model using convLSTM for Hypersonic glide vehicles. In study [32], a prediction method guided by planning using LSTM is proposed. LSTM plays an important role in trajectory prediction [34], [35], [36], however, its long training and prediction times have traditionally been a limitation. To address this issue, [37] proposed a novel attention-enhanced SRU from a cellular unit perspective, which has shown good performance in trajectory prediction. Reference [38] has demonstrated that GRU is more efficient in training and achieves performance similar to LSTM in time-series data regression prediction. Reference [39] proposed a stacked GRU-LSTM network to balance training efficiency and accuracy for solving the parking occupancy time-series prediction problem. All these trajectory prediction models have advanced research in this field in different transportation scenarios. Inspired by [39], [40], and [41], this paper proposes a GRU-LSTM architecture for vehicle trajectory prediction.

B. DECISION-MAKING

In the field of autonomous driving, lane changing is a critical decision that must be made in a timely and safe manner. There are two major approaches to the problem: rule-based models and learning-based models.

Learning-based models, such as imitation learning [42], reinforcement learning [43], RNN and deep reinforcement learning [44], learn decision-making strategies from data. These models can achieve high performance, but they are block-box model, make it difficult to interpret and may require large amounts of training data.

Rule-based models, such as finite state machines [45], model predictive control [46], and fuzzy logic reasoning [47], rely on pre-defined rules to make decisions. While these models are often simple and interpretable, fuzzy logic reasoning has emerged as a promising approach for lane changing decision making in autonomous driving systems [48]. The fuzzy logic model is able to incorporate linguistic rules and expert knowledge, as well as handle uncertainties and imprecise inputs, making it well-suited for real-world driving scenarios [49], [50]. Therefore, another focus of this paper is to design a lane change decision-making model with inferencing ability using fuzzy logical inferencing.

III. METHOD

A. LSTM&GRU-BASED TRAJECTORY PREDICTION

Trajectory prediction is a key factor in decision-making, which predicts the future position of dynamic agents. Recently, LSTM have been considered particularly effective for time series prediction.

Thus, this section provides a detailed process of designing a trajectory prediction model based on LSTM and GRU. Firstly, the input and output layers are modeled; then, the learning layer is established through GRU, LSTM and Fully connected layer. Inspired by citations [39], [40], [41], the GRU is utilized first, which have an effective computing consumption. And then LSTM follows it accounting for the high accurate in regression task. Finally, the loss function designed for training is provided.

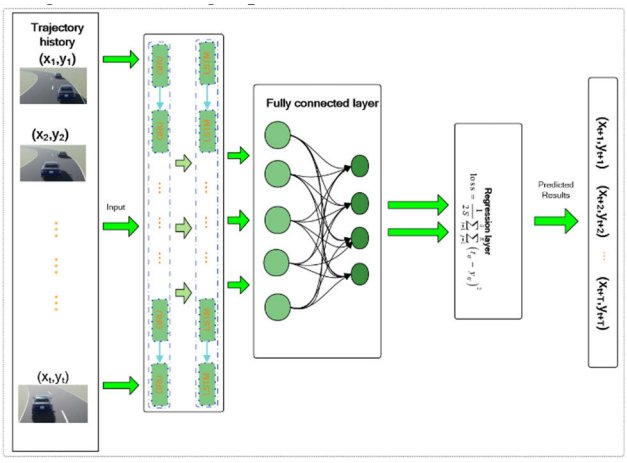

FIGURE 2. Structure of trajectory prediction model.

1) INPUT-OUTPUT

The proposed prediction model is modeled as a ''two-input, two-output'' model. The model's inputs are historical trajectory time series data, represented by:

$$X = [X_{t-m}, X_{t-m+1}, \ldots, X_t] \tag{1}$$

$$X_t = (x_t, y_t) \tag{2}$$

where X_t represents the spatial coordinates, and m is the historical data time window. Setting m equal to 5 is appropriate for the trajectory prediction model used for the hybrid lane-changing decision-making model.

The outputs are represented by:

$$Y = [Y_{t+1}, Y_{t+2}, \cdots, Y_{t+T}] \tag{3}$$

$$Y_{t+T} = (x_{t+T}, y_{t+T}) \tag{4}$$

where Y_{t+T} represents the spatial coordinates, and T represents the prediction duration. Considering that decision-making is short-term inference, we set T is equal to 3 which is adequate for the model's utilization.

2) LEARNING LAYER

The learning layer is primarily composed of GRU, LSTM and fully connected layers. Through the use of GRU and LSTM, historical data can be learned. The GRU is a variant of the LSTM, which removes the short-term memory module and thus can improve processing speed, particularly for large-scale datasets. We utilize its advantages as the first learning layer. The structure of GRU cell is shown in FIGURE 3 a).

Where x_t denotes the input historical trajectory information, h_{t-1} represent the memory content from the previous time step, r_t is the reset gate, z_t is the update gate, $\tilde{h}_t$ is the new memory content, and h_t is the current step's memory content. The core formula is as follows:

$$z_t = \sigma\left(W_z \cdot [h_{t-1}, x_t]\right) \tag{5}$$

$$r_t = \sigma\left(W_r \cdot [h_{t-1}, x_t]\right) \tag{6}$$

$$\tilde{h}_t = \tanh\left(W \cdot [r_t \cdot h_{t-1}, x_t]\right) \tag{7}$$

$$h_t = (1 - z_t) \cdot h_{t-1} + z_t \cdot \tilde{h}_t \tag{8}$$

where x_t represents the input, σ and tanh represent activation functions. W_z denotes the weight matrix for the reset gate, W_r denotes the weight matrix for the update gate, and W denotes the weight matrix for generating new memory content.

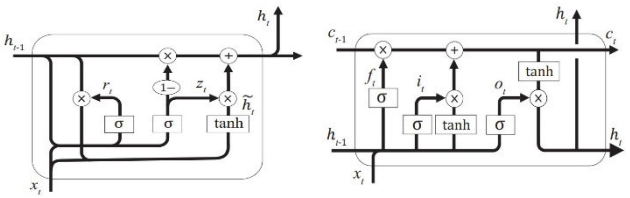

a) GRU cell b) LSTM cell

FIGURE 3. Structure of GRU and LSTM cell.

The structure of LSTM cell is shown in FIGURE 3 b). C_{t-1} and h_{t-1} represent the long-term memory and hidden information from the previous time step, while x_t represents the input event information. In our model, x_t is the input

historical trajectory information, C_t and h_t represent the cell's outputs of long-term memory and hidden information.

For the internal structure of the LSTM cell, the forget gate can be understood as a filter in a recurrent network, wherein the information without positive stimulus for the next learning unit in the recurrent learning process is neglected by the forget gate, and its role in trajectory prediction is to eliminate values that deviate significantly from actual values during the recurrent learning process. The forget gate is implemented as shown in Equation (9).

$$f_t = \sigma\left(W_f \cdot [h_{t-1}, x_t] + b_f\right) \tag{9}$$

where f_t represents the forget gate, W_f is the weight matrix of the forget gate, and b_f is the bias of the forget gate.

The updating of memory information first integrates the input gate information i_t and short-term memory information h_{t-1}. The formula for this process is shown below:

$$i_t = \sigma\left(W_i \cdot [h_{t-1}, x_t] + b_i\right) \tag{10}$$

$$\tilde{C}_t = \tanh\left(W_C \cdot [h_{t-1}, x_t] + b_C\right) \tag{11}$$

where i_t represents the input gate, $\tilde{C}_t$ represents the candidate value vector, W_i and W_C is the weight matrix, b_i and b_C is the bias of the input gate and candidate value vector, respectively.

The output gate processes input information x_t, previous hidden information h_{t-1} and integrates it with the memory information to output h_t. C_t is formed by integrating f_t, C_t and C_{t-1}. The formula for this process is shown below:

$$O_t = \sigma\left(W_o \cdot [h_{t-1}, x_t] + b_o\right) \tag{12}$$

$$C_t = f_t \cdot C_{t-1} + i_t \cdot \tilde{C}_t \tag{13}$$

$$h_t = O_t \cdot \tanh\left(C_t\right) \tag{14}$$

where O_t represents the output gate, C_t represents the output information of this cell, h_t represents the hidden state, W_o is the weight matrix, b_o is the bias of the output gate.

In these procedures, σ and tanh are activation functions, as shown in Equations (15) and (16). σ is sigmoid activation function that range is between 0 and 1, which determines the values that need to be updated. The advantage of the tanh function is its ability to alleviate gradient vanishing and improve training speed.

$$\sigma\left(x\right) = \frac{1}{1 + e^{-x}} \tag{15}$$

$$\tanh\left(x\right) = \frac{e^{x} - e^{-x}}{e^{x} + e^{-x}} \tag{16}$$

For the FCN layer, a fully connected layer is used to multiply the dense input vector matrix with the trainable weight matrix and bias vector outputted by the GRU-LSTM layer, in order to obtain the most suitable network parameters, the specific formula is shown below:

$$\mathrm{Out} = \mathrm{FC}(\mathrm{LSTM}(\mathrm{I_t})) \tag{17}$$

where $\mathrm{I_t}$ is inputs, FC denotes the fully connected layer, Out denotes the final outputs.

3) REGRESSION LAYER

As trajectory prediction is essentially a supervised learning process, it involves iteratively fitting trajectory data through regression. Ultimately, a regression layer is employed as the last layer of the model, allowing the model to progressively fit the data and generate appropriate weights during training. Training Loss function is as follows:

$$\mathrm{loss} = \frac{1}{2S}\sum_{i=1}^{S}\sum_{j=1}^{R}\left(\mathrm{t_{ij}} - \mathrm{y_{ij}}\right)^2 \tag{18}$$

where R represents the number of responses is 2, responses indicate the vehicle position coordinates 'x' and 'y', and S represents the sequence length, t_{ij} represents the predicted value, y_{ij} represents the ground truth.

The activation function between the neural layers of the prediction model is the ReLU function, as shown in Equation (19). The main advantage of using the ReLU over other activation functions is that it does not activate all the neurons at the same time, if the input is negative, it will convert it to zero and the neuron does not get activated.

$$\mathrm{ReLU}(x) = \begin{cases} x, & x > 0 \\ 0, & x \leq 0 \end{cases} \tag{19}$$

The evaluation metric of the prediction model is shown in Equation (20):

$$\mathrm{RMSE} = \sqrt{\frac{1}{2m}\sum_{i=1}^{m}\left(\left(x_i - \hat{x}_i\right)^2 + \left(y_i - \hat{y}_i\right)^2\right)} \tag{20}$$

where x_i and y_i are the ground truth values, $\hat{x}_i$ and $\hat{y}_i$ are the predicted values, and m is the sequence data length. Trajectory prediction experiments and analysis of results are presented in Section IV.

B. DECISION MAKING MODEL

This part focuses on implementing the decision-making process of ego vehicle lane changing while considering the predicted trajectory of the other vehicles. Since the prediction model is a black box and the decision-making process is a nonlinear process that changes with influencing factors, a fuzzy reasoning model is employed to fuse decision-making factors in a probabilistic manner and explicitly reason out the final decision. To optimize the model, targeted parameter tuning is conducted. Firstly, a distance warning model considering the predicted position is established. Then, a lane change prompting model is built based on the relative position and speed relationship between two vehicles. Finally, the lane changing decision-making model is constructed.

The process of passing the lane change intention coefficient through the membership function is called the fuzzy encoding process. The process of transforming the lane change willingness coefficient to get the final decision result is called fuzzy decoding, and we use ''centroid'' method as the fuzzy decoder here.

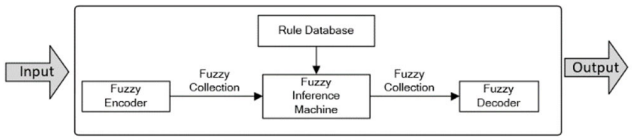

FIGURE 4. Structure of decision-making model.

1) DISTANCE WARNING MODEL

It is necessary to determine a relative distance between vehicles that constitutes an absolute safe distance. When the distance between ego vehicle (EV) and target vehicle (TV) is greater than this threshold, EV may not need to consider the TV's potential driving threats.

The formulas for vehicle kinetic energy and braking work are as follows:

$$\mathrm{E} = \frac{1}{2}mv^2 \tag{21}$$

$$\mathrm{W} = \mu m g d_b \tag{22}$$

where m is the vehicle's mass, v is the vehicle's velocity, μ is the coefficient of friction between the road surface and the tires, g is the gravity of Earth, and d_b is the distance travelled.

According to the law of conservation of energy, setting $\mathrm{E} = \mathrm{W}$, μg as α which represents the maximum deceleration of vehicle (It can be set according to the research scenario, which is set 3 in our research), and d_b can be derived:

$$d_b = \frac{v^2}{2\alpha} \tag{23}$$

Therefore, the distance between two vehicles can be modeled by the following equation:

$$\mathrm{d}'_{\mathrm{w}} = \frac{1}{2\alpha}\left(v_e^2 - v_T^2\right) \tag{24}$$

where v_e is velocity of the ego vehicle, v_T is velocity of target vehicle.

One advantage of automated driving systems is that they can directly control the vehicle through electronic system. Vehicle exits system delay time and human driver reaction time. According to [51], a system delay time of $\tau = 0.2$s has been set to ensure the safety of the system in the event of a computing delay. For human drivers, the delay reaction time is about 1s. Assuming that the driving velocity of the car is 30km/h, it will travel 8.33 meters in 1 second. In order to further ensure the safety of the system, we set a tolerance distance $d_0 = 10$m. So, the final distance warning model formula is as follows:

$$d_w = \frac{1}{2\alpha}\left(v_e^2 - v_T^2\right) + v_e \cdot \tau + d_0 \tag{25}$$

2) LANE CHANGE PROMPTING MODEL

The lane change prompting model is applicable when the distance between two vehicles falls below the safe distance threshold established in distance warning model. In this situation, a driving threat from the other vehicle must be considered. We strive for a smooth and gradual decrease in speed during lane changes, which entails leaving enough distance between vehicles to allow for speed adjustment. Therefore, we develop a lane change prompting model that considering the predicted trajectory, which is represented by d_p.

$$x_1(t) = x_{10} + v_e \cdot t \tag{26}$$

$$x_2(t) = x_{20} + v_T \cdot t - 0.5 \cdot a_T \cdot t^2 \tag{27}$$

Since the ambient vehicle is assumed to be in uniform motion, a_T is set to 0, so the formula is converted to:

$$x_2(t) = x_{20} + v_T \cdot t \tag{28}$$

$$d_p = x_2 - x_1 \tag{29}$$

where x_{10} and x_{20} is the location of EV and TV, x_{20} - x_{10} is equal to the distance between two vehicles. Considering that the front and rear positions of the two vehicles are exchanged after the lane change, it is necessary to take the absolute value of the difference. We adapt the Euclidean distance considering predicted trajectory to formulate the distance between two vehicles as follows:

$$d = \left| \sqrt{(\hat{x}_2 - x_1)^2 + (\hat{y}_2 - y_1)^2} - v_e \cdot t_d \right| \tag{30}$$

where $(\hat{x}_2, \hat{y}_2)$ is the predicted coordinates of TV, (x_1, y_1) are the trajectory coordinates of EV, t_d is the trajectory prediction duration used for decision-making which is set to 1.5 here, considering a system delay time and delay reaction time of human drivers like reference [51].

3) DECISION MAKING MODEL

Based on the safe distance warning model [51] and the lane change prompting model discussed above, we establish a lane change key factor model for the decision-making process. Specifically, this model can be expressed as:

$$w_i = \frac{d - d_p}{d_w - d_p} \tag{31}$$

where w_i represents the key factor value between the i-th pair of vehicles, d, d_p and d_w have described above. The situation $w_i > 1$ corresponds to $d > d_w$. Here, $w_i > 1$ denotes a safe driving distance.

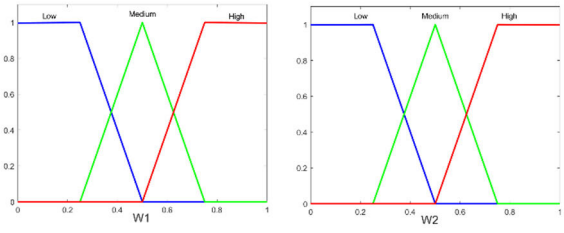

FIGURE 5. Fuzzy input membership functions.

Actually, there is a great nonlinear relationship between the decision of whether the vehicle can change driving state. Fuzzy logic algorithm can better solve the nonlinear system control under complex information. From actual driving

experience, we know that the driving stage changing of vehicles is related to the driving speed and the distance between vehicles. When the speed is high and the distance between vehicles is small, it is easy to cause collision and other dangers. The lane change key factor model is defined here as the input of the fuzzy system. The fuzzy rule base is presented in TABLE 1.

TABLE 1. Fuzzy rule base of model D.

Level marks	Input rule base	Output rule base
Low	0~0.5	0~0.3
Middle	0.25~0.75	0.2~0.8
High	0.5~1	0.6~1

We set up a fuzzy inference rules, which is presented in TABLE 2. w_1 represents the key factor associated with the proximity between the ego vehicle and the leading vehicle in the same lane, whereas w_2 represents the key factor associated with the proximity between the ego vehicle and the obstacle vehicle in the adjacent lane. A smaller value of w_1 indicates a shorter distance between the ego vehicle and the leading vehicle, implying a higher lane-changing intention. Conversely, a larger value of w_2 reflects a greater distance between the ego vehicle and the vehicle in the adjacent lane, also indicating a higher lane-changing intention. To avoid ambiguity, the actual interpretation of w_1 is defined as $1-w_1$, that is $w_1 \Leftarrow 1-w_1$. This ensures a consistent notion where a high value of w indicates that lane changing is recommended. Taking a lane change case with two obstacle vehicles as an example, w_1 and w_2 are taken as the inputs of FIS, w_1 is taken as input1, w_2 is taken as input 2, and the fuzzy membership function is shown in FIGURE 5.

Input the membership function to convert the specific value of the lane change key factor w into fuzzy values, which is represented as low, medium and high, representing the lane change intention decided by the ego vehicle according to the situation of the other vehicle.

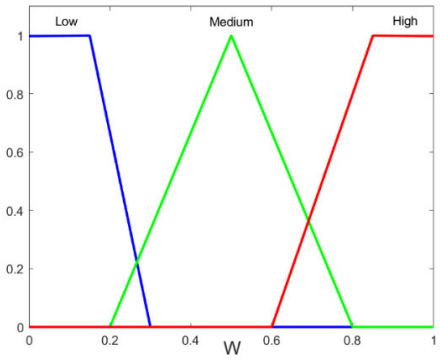

FIGURE 6. Fuzzy output membership functions.

The output membership function represents the relationship between the lane change feasibility and the value processed by the fuzzy rule. Note that when considering a scenario with only FV, we set $w_2 = 1$, indicating that no other car in the left lane poses a driving threat to the EV.

TABLE 2. Fuzzy inference rules.

w		w_1		
		Low	**Medium**	**High**
w_2	**Low**	Low	Low	Medium
	Medium	Low	Medium	High
	High	Low	Medium	High

The three-dimensional thermodynamic change trend is shown in the FIGURE 7. We can see that the w value of the decision model increases with the growth of w_1 and w_2. In fact, from the general trend of the lane change key factor and the relative distance between 2 vehicles, We can see that the w value of the decision model increases with the growth of w_1 and w_2. In this way, w is positively correlated with the change trend of w_1 and w_2, which is reflected in the three-dimensional thermal map and is more obvious for observation.

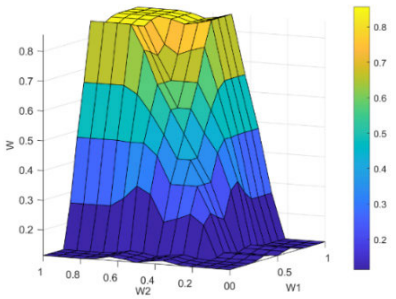

FIGURE 7. 3-dimensional thermodynamic change trend of fuzzy output.

IV. EXPERIMENTS AND RESULTS DISCUSSION

We first test our trajectory prediction model on our collected data, then fine tune on the collected data from simulation scenario. To verify the proposed decision-making model, we built 4 driving cases with 2 sets of contrast decision-making model parameters, and the fuzzy rule base are shown in TABLE 3 and TABLE 4, fuzzy inference rules as same as TABLE 2. Additionally, a bicycle model and fifth-degree polynomial are used for trajectory generation.

TABLE 3. Fuzzy rule base of D1.

Level marks	Input rule base	Output rule base
Low	0~0.4	0~0.2
Middle	0.35~0.65	0.2~0.8
High	0.6~1	0.8~1

TABLE 4. Fuzzy rule base of D2.

Level marks	Input rule base	Output rule base
Low	0~0.6	0~0.4
Middle	0.15~0.85	0.2~0.8
High	0.4~1	0.6~1

A simulation environment for algorithm verification is built based on MATLAB/Simulink, and then a virtual visualization environment with more rendering richness is built based on Unreal Engine, which can help us better observe different model performance.

A. PREDICTION EXPERIMENTS

1) PREDICTED RESULTS

For supervised machine learning methods, data training is crucial for determining appropriate model parameters. However, conventional practice of using public datasets for training, verification, and testing of prediction tasks has limitations. Such datasets may primarily focus on improving the generalization ability of a specific scenario, making it challenging to develop models for other scenarios. Our emphasis in this study is on the practicality and interpretability of the model in specific scenarios, rather than just large-scale datasets. Hence, we conducted data simulation by Automated Driving Toolbox in MATLAB for two scenarios: straight road and curve road. We simulated 1000 road simulations for straight road driving scenario, where the speed ranges from 6m/s to 15m/s and the length ranges from 200 meters to 500 meters. Additionally, as the radius of the curve road is unknown, we simulated 1000 sets of data for curve road to account for this uncertainty, where the radius of curvature ranges from 10m to 50m and the length ranges from 100∼400 meters.

The prediction results of RMSE evaluation metric, as shown in TABLE 5, closely approximate various state-of-the-art (SOTA) [52]. Therefore, our prediction outcomes may offer reliable results for decision-making.

TABLE 5. Prediction horizon.

Method	Scenario	1s	2s	3s
GRU-ONLY	**Straight road**	**1.87**	2.85	3.85
	curve road	2.54	3.92	5.34
LSTM-ONLY	**Straight road**	1.97	2.71	3.52
	curve road	2.97	4.29	5.76
GRU&LSTM	**Straight road**	1.88	**2.56**	**3.35**
	curve road	**1.73**	**2.14**	**2.60**

B. SCENARIO TESTS

The experimental results of velocity and gap indicators are represented by a series of abbreviated names. As illustrated in Figure 8, "EV" represents the ego vehicle, "FV" indicates the preceding vehicle in the same lane as the ego vehicle, and "LV" denotes the preceding vehicle in the left lane adjacent to the ego vehicle. The magnified subfigure within Figure 10 allows us to observe their respective positions clearly. EV&FV denotes the relation between EV and FV, and EV&LV denotes the relation between EV and LV.

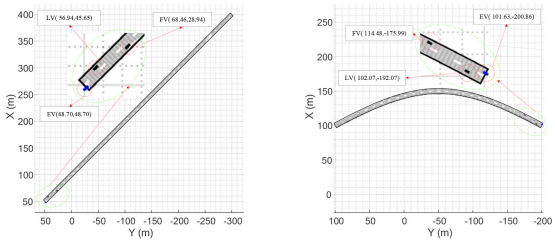

FIGURE 8. Scenario test road.

For more details can be observed in TABLE 6. The suffix 'N' and 'P' respectively indicates the model without or with trajectory prediction, 'D', 'D1' and 'D2' indicates the decision model which parameters configuration can be found in TABLE 2, TABLE 3 and TABLE 4, respectively, where 'D' means the proposed decision-making model, 'D1' and 'D2' are two contrast models.

TABLE 6. Abbreviate explanation.

Abbreviate	Meaning
EV/N-D	EV in the decision model D without trajectory prediction.
EV/P-D	EV in the decision model D with trajectory prediction.
EV&FV/N-D	The relation between EV and FV in the decision model D without trajectory prediction.
EV&FV/P-D	The relation between EV and FV in the decision model D with trajectory prediction.
EV&LV/N-D	The relation between EV and LV in the decision model D without trajectory prediction.
EV&LV/P-D	The relation between EV and LV in the decision model D with trajectory prediction.
EV/P-D1	EV in the decision model D1 with trajectory prediction.
EV&FV/P-D1	The relation between EV and FV in the decision model D1 with trajectory prediction.
EV&LV/P-D1	The relation between EV and FV in the decision model D1 with trajectory prediction.
EV/P-D2	EV in the decision model D2 with trajectory prediction.
EV&FV/P-D2	The relation between EV and FV in the decision model D2 with trajectory prediction.
EV&LV/P-D2	The relation between EV and LV in the decision model D2 with trajectory prediction.

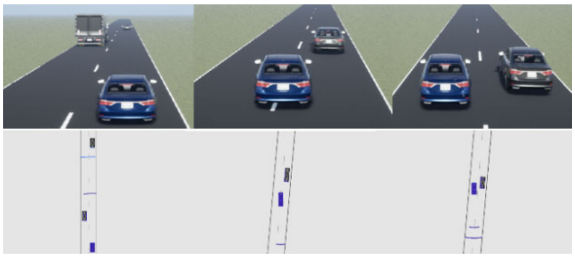

FIGURE 9. Lane changing 3D visualization of case a.

1) CASE A. TWO VEHICLES ON A STRAIGHT ROAD

The EV and the FV are positioned in the right lane. In these conditions, the decision-making parameters for the EV regarding the lane change must consider the existing relationship between the EV and FV.

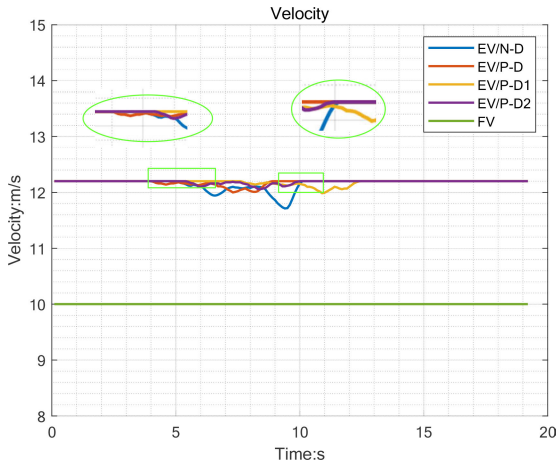

FIGURE 10. Gaps between vehicles of case a.

Based on Figure 10, we can observe that the ego vehicle first decelerates, then accelerates to execute the overtaking maneuver, and returns to cruising speed after completing the lane change. The vehicle modeled with P-D enters the velocity adjustment state at approximately 4 s and completes at around 9 s, with a range from 12 m/s to 12.2 m/s. The lane-changing process takes about 5 seconds to complete. The vehicle modeled with N-D enters the velocity adjustment state slightly later, at approximately 5 s, and completes at around 10 s, with significant fluctuations in a range from 11.7 m/s to 12.2 m/s. The vehicle modeled with P-D1 enters the velocity adjustment state the latest, the adjustment range is the smallest, and the adjustment time is the shortest, which means that the velocity under this model is the fastest, this is very similar to the aggressive style of driver. Under P-D2 mode, the overall jitter of the lane change velocity is not large, but it has been in a state of jitter throughout the whole lane change process, especially when the adjustment is about to be completed at the end, it suddenly jitters. Continual jerky velocity takes a toll on comfort.

Furthermore, FIGURE 11 illustrates the variation of the gap changes of the EV and the FV under the 4 models. The gap curves begin to diverge at around 4 s, which corresponds to the time difference in the velocity variations. The completion time of EV under P-D model and P-D2 model is relatively close, at about 12 s. In P-D1 mode, due to its fast velocity, the lane change behavior is completed at the earliest, at about 11 s. This means that although the velocity adjustment time lags behind in this mode, due to the high velocity, the lane changing task can be completed earlier. Under N-D model, this is the latest to complete lane change, at about 12.5 s. Due to its large velocity jitter and the time to complete the lane change is late, this mode is the least efficient. Note that a

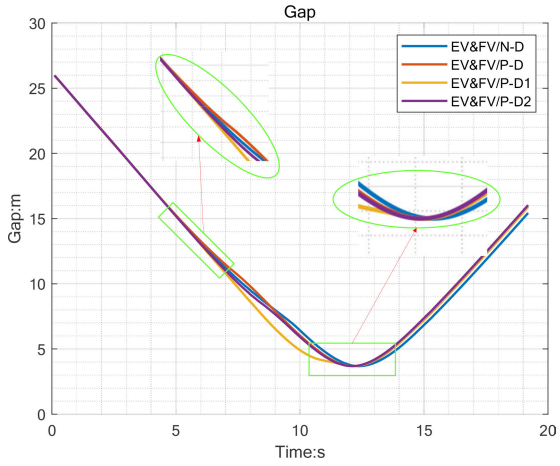

FIGURE 11. Gaps between vehicles of case a.

speed differential between 2 vehicles causes the gap changing trend.

In summary, our proposed decision-making model enables vehicle to execute lane changes at a smoother velocity. In terms of human driving behavior, human driver would anticipate the positions of the front vehicle before making a lane change. In scenarios where there are no vehicles in the neighboring lane, human driver would adjust their speed beforehand to complete the maneuver at a moderate pace, taking into account both driving safety and comfort. Additionally, all models demonstrate similar driving efficiency, as evidenced by the comparable duration of the minimum gap between the EV and FV.

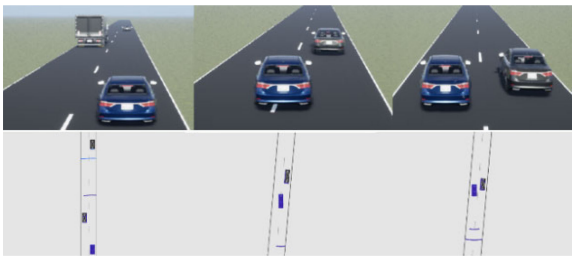

FIGURE 12. Lane changing 3D visualization of case b.

2) CASE B. THREE VEHICLES ON A STRAIGHT ROAD

The EV and the FV are positioned in the right lane, with the LV located in the left lane to the left front of the ego vehicle and the left rear of the front vehicle. In this context, the EV's decision-making factors for changing lanes must take into account not only the FV but also the LV.

Based on the velocity graph displayed in FIGURE 13, upon implementation of P-D model, the vehicle entered a state of velocity adjustment at approximately 12 s, initiated deceleration at approximately 15.2 s, concluded deceleration at 16 s, experiencing a decrease in velocity from 12.2 m/s to 11.8 m/s, and then proceeded to accelerate. Ultimately,

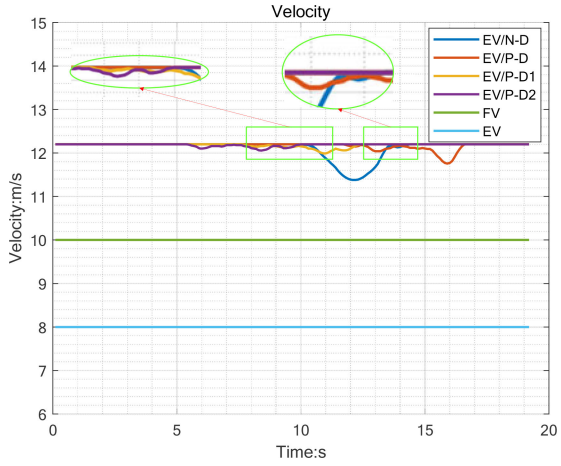

FIGURE 13. Velocity changes of case b.

the adjustment phase was completed at approximately 16.5 s, concluding with a velocity of 12.2 m/s, and resulting in a velocity adjustment lasting approximately 4.5 seconds. The vehicle with N-D model began decelerating at around 10.2 s, ceased deceleration at approximately 12 s, concluded acceleration at around 13.5 s, underwent a slight adjustment for roughly 0.5 seconds, and completed velocity alteration at 14 s. In total, the velocity modification process lasted around 4.8 seconds. The magnitude of velocity adjustment in model P-D1 and P-D2 is small, indicating no significant deceleration during lane changing. From the perspective of human drivers, this strategy is aggressive. Although it leads to high lane changing efficiency, there may be potential safety threats.

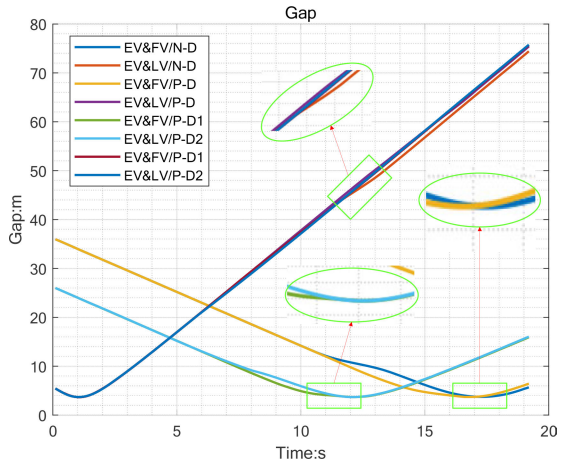

FIGURE 14. Gaps between vehicles of case b.

FIGURE 14 presents the gap graph which illustrates the relative distances among three vehicles: EV, FV, and LV. The P-D model enabled the EV to approach the FV gradually, with the gap value reaching a minimum at 17 s, indicating a completed lane change, and subsequently increasing as the EV moved away from the FV. The vehicle modeled with N-D reached its minimum gap value at 18 s, followed by a gradual increase in the gap value as the EV moved further away from the FV. Under 4 models, the gap between EV and LV reached its minimum at 2 s and then began to increase, indicating a change in proximity from far to close and then back to far, consistent with speed profiles. The magnitude of speed adjustment is small, allowing EV to quickly approach LV and leave. EV has the earliest time point for completing lane changing due to the relatively fast velocity.

In brief, our proposed model directs the vehicle to perform a lane change at an even velocity when confronted with two obstacle vehicles (FV and LV). This application of P-D model process facilitates more rational driving for the EV.

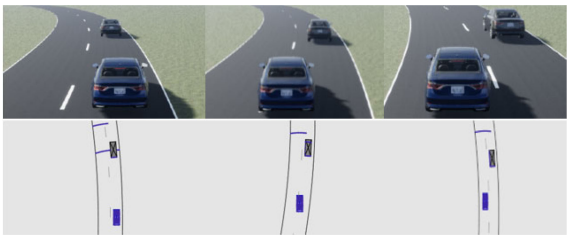

FIGURE 15. Lane changing 3D visualization of case c.

3) CASE C. TWO VEHICLES ON A CURVED ROAD

The EV and the FV are positioned in the right lane. In these conditions, the decision-making parameters for the EV regarding the lane change must consider the existing relationship between the EV and FV.

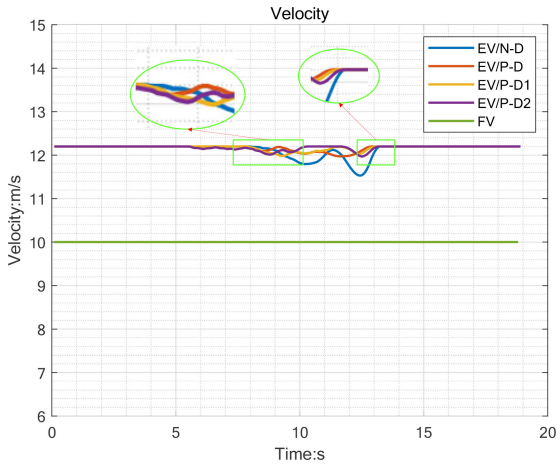

FIGURE 16. Velocity changes of case c.

FIGURE 16 illustrates that the utilization of P-D model in the vehicle induces a velocity adjustment state at approximately 8 s and concludes at around 12.8 s, with a speed change ranging from 12 m/s to 12.2 m/s. The decision-making process for the adjustment takes about 4.8 seconds. In contrast, the vehicle with N-D model exhibits a marginally deferred deceleration directive, as it enters the adjustment state at roughly 8.5 s and completes at around 13.2 s. The velocity change ranges from 11.5 m/s to 12.2 m/s, displaying

prominent fluctuations with a total duration of approximately 4.7 seconds. The velocity variation in the first half of P-D1 model is almost identical to P-D model, except for a minor velocity adjustment at around 11 s. EV with P-D2 model starts adjusting from 5.5 s and completes by 13 s. It enters a similar state of slight velocity adjustment as P-D1 model and eventually completes the adjustment during the lane changing process.

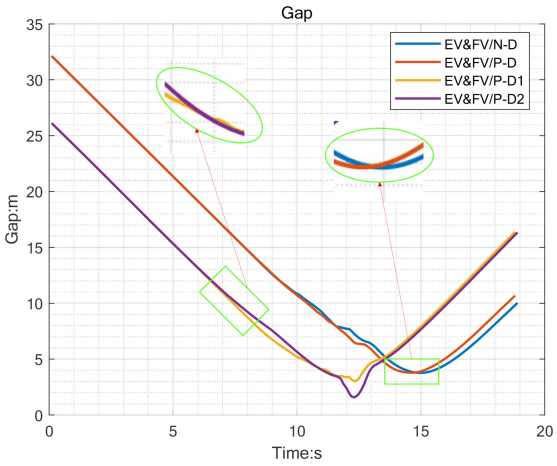

FIGURE 17. Gaps between vehicles of case c.

FIGURE 17 illustrates the gap changes. Notably, there is a clear difference in the gap trends under the 4 methods. Deviations in their speed change times begin to manifest at approximately 7 s, causing the gap values to diverge. Specifically, the resultant gap value for P-D model reaches its lowest point at 15 s, whereas the corresponding metric for the vehicle modeled with N-D reaches its lowest point at 14.5 s before gradually increasing as the EV progressively moves away from the FV, it seems too cautious. Vehicle gap curves of P-D1 and P-D2 model correspond to the velocity profiles. Due to a short-term fine adjustment during the final stage of velocity adjustment, there is a sudden change in distance between vehicles, indicating that either overly cautious or aggressive driving style are unfavorable for driving safety and comfort.

In conclusion, the proposed method enables vehicle to make a smoother velocity adjustment while navigating a curved road with only a front obstacle vehicle. Consequently, the method effectively facilitates a timely and efficient lane change, as evidenced by the attainment of minimum gap values and velocity adjustment time between the EV and FV. Moreover, the proposed model also enhances comfort levels, affirming its effectiveness in achieving dual objectives.

4) CASE D. THREE VEHICLES ON A CURVED ROAD

The EV and the FV are situated in the right lane, while the LV is located in the left lane ahead of the ego vehicle. The lane-changing lane change process is influenced by factors such as the presence of the FV in the ego vehicle's lane and the LV in the adjacent lane.

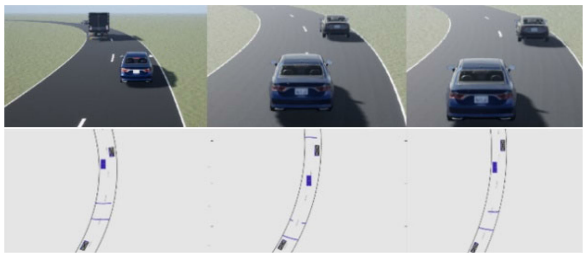

FIGURE 18. Lane changing 3D visualization of case d.

Based on the data presented in FIGURE 19, it is apparent that the vehicle modeled with P-D enters into the velocity adjustment state at approximately 8 s. During the time period between 8 s and 9 s, the variation in velocity is minimal. The process of velocity adjustment concludes at approximately 13.2 s, with a shift in velocity ranging from 11.7m/s to 12.2m/s. The decision-making process itself requires roughly 5.2 seconds to complete. By contrast, the deceleration of the vehicle equipped with N-D model begins slightly later, entering into the speed adjustment state at around 9.8 s, and concluding the adjustment process at roughly 14.2 s. The range of velocity variation during this time period is between 10.8m/s and 12.2m/s. Notably, the adjustment in velocity is greater, and the overall process of velocity change lasts approximately 4.4 seconds. Vehicle modeled with P-D2 enters the adjustment state earliest, with a relatively long time for velocity adjustment, from 5.5 s to 13 s. Vehicle modeled with P-D1 enters velocity adjustment later. After going through the process of decreasing and increasing velocity, vehicle modeled with P-D1 or P-D2 experiences short-term velocity fluctuations in the final stage.

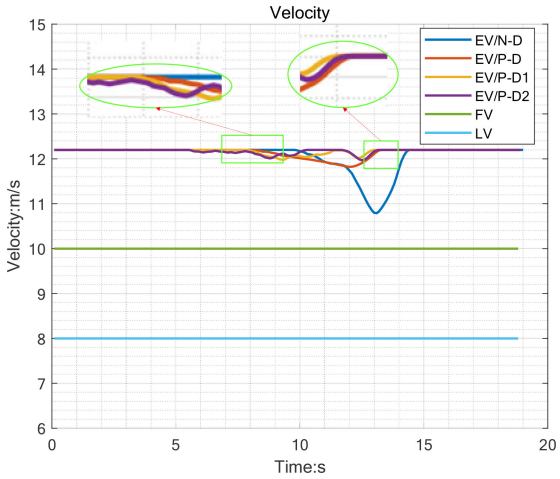

FIGURE 19. Velocity changes of case d.

FIGURE 20 illustrates the variation of the gap value. Notably, at approximately 7 s, a significant disparity in the gap trends emerged among the 4 methods, coinciding with the variance in their velocity changes. The gap value between the EV and LV decreased to its minimum at 1.3 s,

signifying the closest proximity between the two vehicles. Subsequently, the gap between the vehicles widened, leading to an increment in the gap parameter. The vehicle modeled with P-D recorded the least gap value at 16.5 s, compared to N-D model, which attained the minimum gap value at 17 s. Because the velocity is relatively high during lane changing under P-D1 or P-D2, EV completes lane changing relatively early, at 12.5 s and 12.2 s respectively, consistent with the speed profiles. Gap values between EV and LV are similar across different methods.

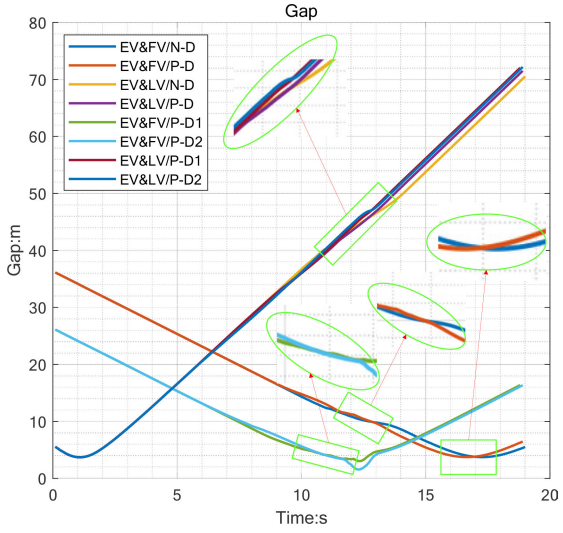

FIGURE 20. Gaps between vehicles of case d.

In summary, when facing a scenario on a curved road with EV, LV and FV, our proposed decision-making model can guide the vehicle to change lanes at a smoother speed. Additionally, the time it takes for the gap value between the EV and FV to diminish to the minimum value is half a second faster than N-D model. While P-D1 model and P-D2 model performs too aggressive.

V. CONCLUSION

This study presents a lane-changing decision model that accounts for trajectory prediction to enhance driving comfort and ensure driving safety. Initially, a trajectory prediction model is established to guarantee accurate trajectory prediction. Subsequently, to ensure the reliability of the decision reasoning model, we design a distance warning model, a lane change prompting model, a key factor model, and a decision-making model. Fuzzy rules are created for fuzzy inference decision based on these models. Finally, the proposed method's effectiveness is validated through four case studies, which reveal our model can substantially ensure driving safety and improve comfort with minimal loss of driving efficiency. In the future, we will optimize the proposed deep learning model with the goal of generating long-term decision tasks for complex traffic environments through training strategies such as imitation learning.

REFERENCES

[1] H. Su and Y. Jia, "Study of human comfort in autonomous vehicles using wearable sensors," *IEEE Trans. Intell. Transp. Syst.*, vol. 23, no. 8, pp. 11490–11504, Aug. 2022.

[2] W. B. Qin, "A nonlinear car-following controller design inspired by human-driving behaviors to increase comfort and enhance safety," *IEEE Trans. Veh. Technol.*, vol. 71, no. 8, pp. 8212–8224, Aug. 2022.

[3] O. Sharma, N. C. Sahoo, and N. B. Puhan, "Kernelized convolutional transformer network based driver behavior estimation for conflict resolution at unsignalized roundabout," *ISA Trans.*, vol. 133, pp. 13–28, Feb. 2023.

[4] O. Sharma, N. C. Sahoo, and N. B. Puhan, "Recent advances in motion and behavior planning techniques for software architecture of autonomous vehicles: A state-of-the-art survey," *Eng. Appl. Artif. Intell.*, vol. 101, May 2021, Art. no. 104211.

[5] M. R. Siddiqi, S. Milani, R. N. Jazar, and H. Marzbani, "Motion sickness mitigating algorithms and control strategy for autonomous vehicles," *IEEE Trans. Intell. Transp. Syst.*, vol. 24, no. 1, pp. 304–315, Jan. 2023.

[6] Y. Ma, C. Sun, J. Chen, D. Cao, and L. Xiong, "Verification and validation methods for decision-making and planning of automated vehicles: A review," *IEEE Trans. Intell. Vehicles*, vol. 7, no. 3, pp. 480–498, Sep. 2022.

[7] A. Duz, A. Gimondi, M. Corno, and S. M. Savaresi, "An efficient eco-planner for autonomous vehicles with focus on passengers comfort," *IEEE Trans. Veh. Technol.*, vol. 71, no. 7, pp. 6984–6995, Jul. 2022.

[8] H. Gao, Y. Qin, C. Hu, Y. Liu, and K. Li, "An interacting multiple model for trajectory prediction of intelligent vehicles in typical road traffic scenario," *IEEE Trans. Neural Netw. Learn. Syst.*, vol. 34, no. 9, pp. 6468–6479, Sep. 2023.

[9] O. Sharma, N. C. Sahoo, and N. B. Puhan, "A survey on smooth path generation techniques for nonholonomic autonomous vehicle systems," in *Proc. 45th Annu. Conf. IEEE Ind. Electron. Soc. (IECON)*, vol. 1, Oct. 2019, pp. 5167–5172.

[10] M. Fu, T. Zhang, W. Song, Y. Yang, and M. Wang, "Trajectory prediction-based local spatio-temporal navigation map for autonomous driving in dynamic highway environments," *IEEE Trans. Intell. Transp. Syst.*, vol. 23, no. 7, pp. 6418–6429, Jul. 2022.

[11] O. Sharma, N. C. Sahoo, and N. B. Puhan, "Highway discretionary lane changing behavior recognition using continuous and discrete hidden Markov model," in *Proc. IEEE Int. Intell. Transp. Syst. Conf. (ITSC)*, Sep. 2021, pp. 1476–1481.

[12] O. Sharma, N. C. Sahoo, and N. B. Puhan, "Highway lane-changing prediction using a hierarchical software architecture based on support vector machine and continuous hidden Markov model," *Int. J. Intell. Transp. Syst. Res.*, vol. 20, no. 2, pp. 519–539, Jun. 2022.

[13] S. Su, K. Muelling, J. Dolan, P. Palanisamy, and P. Mudalige, "Learning vehicle surrounding-aware lane-changing behavior from observed trajectories," in *Proc. IEEE Intell. Vehicles Symp. (IV)*, Jun. 2018, pp. 1412–1417.

[14] Y. Huang, J. Du, Z. Yang, Z. Zhou, L. Zhang, and H. Chen, "A survey on trajectory-prediction methods for autonomous driving," *IEEE Trans. Intell. Vehicles*, vol. 7, no. 3, pp. 652–674, Sep. 2022.

[15] M. Brännström, E. Coelingh, and J. Sjöberg, "Model-based threat assessment for avoiding arbitrary vehicle collisions," *IEEE Trans. Intell. Transp. Syst.*, vol. 11, no. 3, pp. 658–669, Sep. 2010.

[16] P. Lytrivis, G. Thomaidis, and A. Amditis, "Cooperative path prediction in vehicular environments," in *Proc. 11th Int. IEEE Conf. Intell. Transp. Syst.*, Oct. 2008, pp. 803–808.

[17] S. Liu, H. Liu, H. Bi, and T. Mao, "CoL-GAN: Plausible and collision-less trajectory prediction by attention-based GAN," *IEEE Access*, vol. 8, pp. 101662–101671, 2020.

[18] C. Shen, Y. Yin, X. Wang, X. Li, J. Song, and M. Song, "Training generative adversarial networks in one stage," in *Proc. IEEE/CVF Conf. Comput. Vis. Pattern Recognit. (CVPR)*, Jun. 2021, pp. 3349–3359.

[19] S. Kim, D. Kum, and J. W. Choi, "RECUP Net: RECUrsive prediction network for surrounding vehicle trajectory prediction with future trajectory feedback," in *Proc. IEEE 23rd Int. Conf. Intell. Transp. Syst. (ITSC)*, Sep. 2020, pp. 1–6.

[20] Z. Hao, X. Huang, K. Wang, M. Cui, and Y. Tian, "Attention-based GRU for driver intention recognition and vehicle trajectory prediction," in *Proc. 4th CAA Int. Conf. Veh. Control Intell. (CVCI)*, Dec. 2020, pp. 86–91.

[21] C. Chen, L. Liu, S. Wan, X. Hui, and Q. Pei, "Data dissemination for Industry 4.0 applications in Internet of Vehicles based on short-term traffic prediction," *ACM Trans. Internet Technol.*, vol. 22, no. 1, pp. 1–18, Oct. 2021.
[22] C. Chen, Z. Liu, S. Wan, J. Luan, and Q. Pei, "Traffic flow prediction based on deep learning in Internet of Vehicles," *IEEE Trans. Intell. Transp. Syst.*, vol. 22, no. 6, pp. 3776–3789, Jun. 2021.
[23] Z. Ding, Z. Yao, and H. Zhao, "RA-GAT: Repulsion and attraction graph attention for trajectory prediction," in *Proc. IEEE Int. Intell. Transp. Syst. Conf. (ITSC)*, Sep. 2021, pp. 734–741.
[24] Y. Cai, Z. Wang, H. Wang, L. Chen, Y. Li, M. A. Sotelo, and Z. Li, "Environment-attention network for vehicle trajectory prediction," *IEEE Trans. Veh. Technol.*, vol. 70, no. 11, pp. 11216–11227, Nov. 2021.
[25] K. Messaoud, I. Yahiaoui, A. Verroust-Blondet, and F. Nashashibi, "Attention based vehicle trajectory prediction," *IEEE Trans. Intell. Vehicles*, vol. 6, no. 1, pp. 175–185, Mar. 2021.
[26] Y. Wu, G. Chen, Z. Li, L. Zhang, L. Xiong, Z. Liu, and A. Knoll, "HSTA: A hierarchical spatio-temporal attention model for trajectory prediction," *IEEE Trans. Veh. Technol.*, vol. 70, no. 11, pp. 11295–11307, Nov. 2021.
[27] L. Ye, Z. Wang, X. Chen, J. Wang, K. Wu, and K. Lu, "GSAN: Graph self-attention network for learning spatial–temporal interaction representation in autonomous driving," *IEEE Internet Things J.*, vol. 9, no. 12, pp. 9190–9204, Jun. 2022.
[28] X. Chen, H. Zhang, F. Zhao, Y. Hu, C. Tan, and J. Yang, "Intention-aware vehicle trajectory prediction based on spatial–temporal dynamic attention network for Internet of Vehicles," *IEEE Trans. Intell. Transp. Syst.*, vol. 23, no. 10, pp. 19471–19483, Oct. 2022.
[29] H. Guo, Q. Meng, D. Cao, H. Chen, J. Liu, and B. Shang, "Vehicle trajectory prediction method coupled with ego vehicle motion trend under dual attention mechanism," *IEEE Trans. Instrum. Meas.*, vol. 71, pp. 1–16, 2022.
[30] D. Kim, H. Shon, N. Kweon, S. Choi, C. Yang, and K. Huh, "Driving style-based conditional variational autoencoder for prediction of ego vehicle trajectory," *IEEE Access*, vol. 9, pp. 169348–169356, 2021.
[31] M. Á. D. Miguel, J. M. Armingol, and F. García, "Vehicles trajectory prediction using recurrent VAE network," *IEEE Access*, vol. 10, pp. 32742–32749, 2022.
[32] J. Zhang, J. Xiong, L. Li, Q. Xi, X. Chen, and F. Li, "Motion state recognition and trajectory prediction of hypersonic glide vehicle based on deep learning," *IEEE Access*, vol. 10, pp. 21095–21108, 2022.
[33] Q. Dong, T. Jiang, T. Xu, and Y. Liu, "Graph-based planning-informed trajectory prediction for autonomous driving," in *Proc. 6th CAA Int. Conf. Veh. Control Intell. (CVCI)*, Oct. 2022, pp. 598–614.
[34] T. Zhao, Y. Xu, M. Monfort, W. Choi, C. Baker, Y. Zhao, Y. Wang, and Y. N. Wu, "Multi-agent tensor fusion for contextual trajectory prediction," in *Proc. IEEE/CVF Conf. Comput. Vis. Pattern Recognit. (CVPR)*, Jun. 2019, pp. 12118–12126.
[35] H. He, H. Dai, and N. Wang, "UST: Unifying spatio-temporal context for trajectory prediction in autonomous driving," in *Proc. IEEE/RSJ Int. Conf. Intell. Robots Syst. (IROS)*, Oct. 2020, pp. 5962–5969.
[36] N. Deo and M. M. Trivedi, "Multi-modal trajectory prediction of surrounding vehicles with maneuver based LSTMs," in *Proc. IEEE Intell. Vehicles Symp. (IV)*, Jun. 2018, pp. 1179–1184.
[37] Y. Li, B. Liu, L. Zhang, S. Yang, C. Shao, and D. Son, "Fast trajectory prediction method with attention enhanced SRU," *IEEE Access*, vol. 8, pp. 206614–206621, 2020.
[38] J. Chung, C. Gulcehre, K. Cho, and Y. Bengio, "Empirical evaluation of gated recurrent neural networks on sequence modeling," in *Proc. NIPS Workshop Deep Learn.*, Dec. 2014, pp. 1–9.
[39] C. Zeng, C. Ma, K. Wang, and Z. Cui, "Parking occupancy prediction method based on multi factors and stacked GRU-LSTM," *IEEE Access*, vol. 10, pp. 47361–47370, 2022.
[40] N. Zafar, I. U. Haq, H. Sohail, J.-U.-R. Chughtai, and M. Muneeb, "Traffic prediction in smart cities based on hybrid feature space," *IEEE Access*, vol. 10, pp. 134333–134348, 2022.
[41] A. H. A. Hussain, M. A. Taher, O. A. Mahmood, Y. I. Hammadi, R. Alkanhel, A. Muthanna, and A. Koucheryavy, "Urban traffic flow estimation system based on gated recurrent unit deep learning methodology for Internet of Vehicles," *IEEE Access*, vol. 11, pp. 58516–58531, 2023.
[42] Z. Cheng, L. Liu, A. Liu, H. Sun, M. Fang, and D. Tao, "On the guaranteed almost equivalence between imitation learning from observation and demonstration," *IEEE Trans. Neural Netw. Learn. Syst.*, vol. 34, no. 2, pp. 677–689, Feb. 2023.
[43] S. Mo, X. Pei, and C. Wu, "Safe reinforcement learning for autonomous vehicle using Monte Carlo tree search," *IEEE Trans. Intell. Transp. Syst.*, vol. 23, no. 7, pp. 6766–6773, Jul. 2022.
[44] Y. Tian, X. Cao, K. Huang, C. Fei, Z. Zheng, and X. Ji, "Learning to drive like human beings: A method based on deep reinforcement learning," *IEEE Trans. Intell. Transp. Syst.*, vol. 23, no. 7, pp. 6357–6367, Jul. 2022.
[45] S. Hwang, K. Lee, H. Jeon, and D. Kum, "Autonomous vehicle cut-in algorithm for lane-merging scenarios via policy-based reinforcement learning nested within finite-state machine," *IEEE Trans. Intell. Transp. Syst.*, vol. 23, no. 10, pp. 17594–17606, Oct. 2022.
[46] M. Ammour, R. Orjuela, and M. Basset, "A MPC combined decision making and trajectory planning for autonomous vehicle collision avoidance," *IEEE Trans. Intell. Transp. Syst.*, vol. 23, no. 12, pp. 24805–24817, Dec. 2022.
[47] D. F. Llorca, V. Milanes, I. P. Alonso, M. Gavilan, I. G. Daza, J. Perez, and M. Á. Sotelo, "Autonomous pedestrian collision avoidance using a fuzzy steering controller," *IEEE Trans. Intell. Transp. Syst.*, vol. 12, no. 2, pp. 390–401, Jun. 2011.
[48] W. Wang, T. Qie, C. Yang, W. Liu, C. Xiang, and K. Huang, "An intelligent lane-changing behavior prediction and decision-making strategy for an autonomous vehicle," *IEEE Trans. Ind. Electron.*, vol. 69, no. 3, pp. 2927–2937, Mar. 2022.
[49] X. Xia, P. Hang, N. Xu, Y. Huang, L. Xiong, and Z. Yu, "Advancing estimation accuracy of sideslip angle by fusing vehicle kinematics and dynamics information with fuzzy logic," *IEEE Trans. Veh. Technol.*, vol. 70, no. 7, pp. 6577–6590, Jul. 2021.
[50] C. Huang, P. Hang, Z. Hu, and C. Lv, "Collision-probability-aware human-machine cooperative planning for safe automated driving," *IEEE Trans. Veh. Technol.*, vol. 70, no. 10, pp. 9752–9763, Oct. 2021.
[51] P. Seiler, B. Song, and J. K. Hedrick, "Development of a collision avoidance system," *SAE Trans. Int. J. Passenger Cars*, vol. 107, no. 6, pp. 1334–1340, 1998.
[52] N. Deo and M. M. Trivedi, "Convolutional social pooling for vehicle trajectory prediction," in *Proc. IEEE/CVF Conf. Comput. Vis. Pattern Recognit. Workshops (CVPRW)*, Jun. 2018, pp. 1549–1558.

XUDONG WANG received the M.S. degree in mechanical engineering from the Beijing University of Posts and Telecommunication, Beijing, China, in 2020. He is currently pursuing the Ph.D. degree in mechanical engineering with the Beijing Institute of Technology, Beijing. His current research interests include trajectory prediction and prediction-based decision-making for autonomous vehicle.

JIBIN HU received the Ph.D. degree from the Beijing Institute of Technology, in 2003. He was a Visiting Scholar with Wayne State University. He is currently a Professor with the Beijing Institute of Technology. He is also the Vice Director of the National Key Laboratory of Vehicular Transmission, Beijing Institute of Technology. His current research interests include vehicle dynamics control and transmission control of hybrid vehicle.

CHAO WEI received the Ph.D. degree in mechanical engineering from the Beijing Institute of Technology (BIT), Beijing, China, in 2007. Then, he joined as a Lecturer with BIT, where he is currently a Professor with the Institute of Special Vehicles, School of Mechanical Engineering. He serves as the Vice Director for the Institute of Special Vehicles. His current research interests include vehicle dynamics control and intelligent vehicles.

LUHAO LI was born in Shijiazhuang, Hebei, China, in 1988. He received the master's degree in vehicle engineering from Jilin University, in July 2015. He is currently a Senior Engineer with the Technology Research and Development Center of eDrive Special Vehicles, Beijing Institute of Space Launch Technology. His current research interests include unmanned ground vehicles, and decision making and control.

YONGLIANG LI was born in Chongqing, China, in 1995. He received the master's degree in vehicle engineering from the Beijing Institute of Technology, in July 2021. He is currently an Engineer with the Technology Research and Development Center of eDrive Special Vehicles, Beijing Institute of Space Launch Technology. His current research interests include unmanned ground vehicles, path planning, and decision making and control.

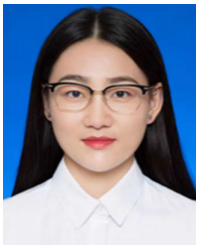

MIAOMIAO DU was born in Nanyang, Henan, China, in 1993. She received the Ph.D. degree in vehicle engineering from Jilin University, in July 2021. She is currently an Engineer with the Technology Research and Development Center of eDrive Special Vehicles, Beijing Institute of Space Launch Technology. Her current research interests include unmanned ground vehicles, and decision making and control.